Electronic Supplementary Material (ESI) for Chemical Science.
This journal is © The Royal Society of Chemistry 2023

Electronic Supplementary Information for

Tailoring High Brightness "Warm" White-light Emission of Two-Dimensional Perovskite Crystals via Pressure Inhibition Nonradiative Transition

Yuanyuan Fang[a], Jingtian Wang[a], Long Zhang[a], Guangming Niu[b], Laizhi Sui[b*], Guorong Wu[b], Kaijun Yuan[b], Kai Wang[a,c*] and Bo Zou[a*]

[a] State Key Laboratory of Superhard Materials, College of Physics, Jilin University, Changchun 130012, China. E-mail: kaiwang@jlu.edu.cn; zoubo@jlu.edu.cn
[b] State Key Laboratory of Molecular Reaction Dynamics, Dalian Institute of Chemical Physics, Chinese Academy of Sciences, 457 Zhongshan Road, Dalian 116023, China. E-mail: lzsui@dicp.ac.cn
[c] Shandong Key Laboratory of Optical Communication Science and Technology, School of Physics Science and Information Technology, Liaocheng University, Liaocheng 252000, China.
*Corresponding Author: kaiwang@jlu.edu.cn; zoubo@jlu.edu.cn; lzsui@dicp.ac.cn.

EXPERIMENTAL DETAILS

Sample preparation

The $(2meptH_2)PbCl_4$ crystals were synthesized according to the method that has previously been reported in the literature.[1] Firstly, $PbAc_2 \cdot 3H_2O$ (1.897 g, 5.0 mmol) was dissolved in 20 ml of 38% hydrochloric acid solution. Then, 2-methyl-1,5-diaminopentane (0.581 g, 5.0 mmol) was added to the solution under stirring and heating. Colorless particles were obtained upon cooling to ambient temperature, and dried overnight under 30 Pa pressure with vacuum.

High Pressure

A diamond anvil cell (DAC) with 400 μm diameter culets was used to reach high pressure conditions. A T301 stainless steel gasket with a 125 μm hole and 40 μm thickness served as the sample chamber. The sample was loaded into the sample chamber along with a ruby ball to determine pressure according to the ruby fluorescence technique. In high pressure optical absorption, PL and XRD experiments, we used silicone oil as a pressure-transmitting medium.

In situ high-pressure optical measurements

The *in situ* high-pressure PL measurements were carried out using the 355 nm line of a UV DPSS laser. *In situ* high-pressure UV-Vis absorption measurements were performed by a deuterium-halogen light source. The fiber spectrometer is an Ocean Optics QE65000 spectrometer. The PL micrographs of the samples upon compression were taken with a camera (CanonEos 5D mark II) installed on a microscope (Ecilipse TI-U, Nikon). *In situ* high pressure infrared absorption measurements were carried out using Nicolet iN10 FT-IR Spectrometer (Thermo Fisher Scientific).

In situ high-pressure time-resolved PL measurements.

Time resolved PL of perovskite in diamond anvil cell were measured by home-made setup. A 375 nm pulsed diode laser (LDH-P-C-375B, 40 ps) was used as excitation source. A 20× ultraviolet objective lens was used to project the incident laser onto the sample and collet the backscattered emission signal. The PL signal was directed into the 500 mm focal length grating spectrograph (HRS-500 MS), where a PMT together with a time correlated single photon counting electronics (TimeHarp 260 PICO) was used to detect the PL kinetics.

Synchrotron radiation XRD

In situ high-pressure angle-dispersive XRD measurements (λ= 0.6199 Å) were performed at the 4W2 High Pressure Station in Beijing Synchrotron Radiation Facility. CeO_2 was used for calibration. All the high-pressure experiments were conducted at room temperature. The diffraction patterns were integrated into one-dimensional profile using the Fit2D program. The Reflex module combined in Materials Studio was used for Rietveld refinement.

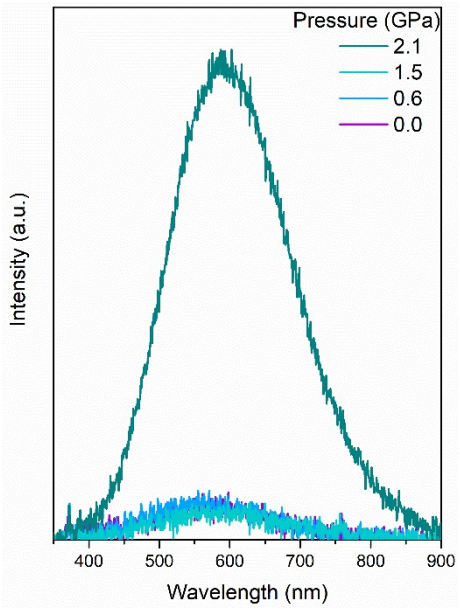

Figure S1. PL spectra of $(2meptH_2)PbCl_4$ crystal at selected pressure below 2.1 GPa.

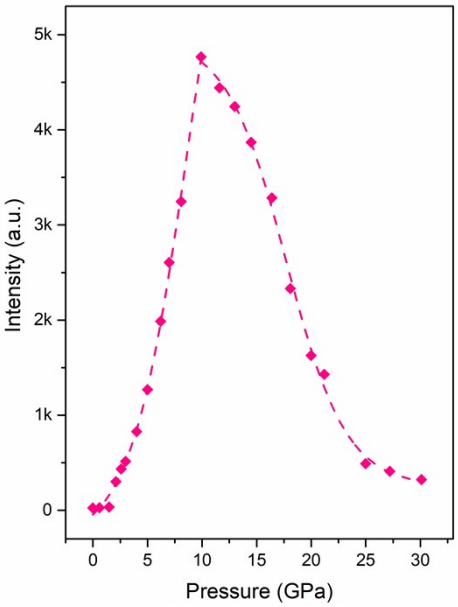

Figure S2. Variations in the PL intensity of $(2meptH_2)PbCl_4$ as a function of pressure excited by 355 nm ultraviolet light.

Table S1 Color scale and color temperature values corresponding to photoluminescence spectra under different pressures

Pressure（GPa）	CIE X	CIE Y	Color Temperature (K)
0.0	0.3872	0.4174	4097
1.5	0.4022	0.4279	3834
2.1	0.4324	0.4505	3419
3.0	0.4301	0.4518	3465
4.0	0.4295	0.4542	3491
5.0	0.4285	0.4553	3516
6.2	0.4300	0.4567	3499
7.0	0.4283	0.4570	3528
8.1	0.4304	0.4577	3499
9.9	0.4244	0.4571	3597
13.0	0.4114	0.4537	3805
18.1	0.3923	0.4330	4072
20.2	0.3871	0.4240	4136
30.1	0.3771	0.4061	4275

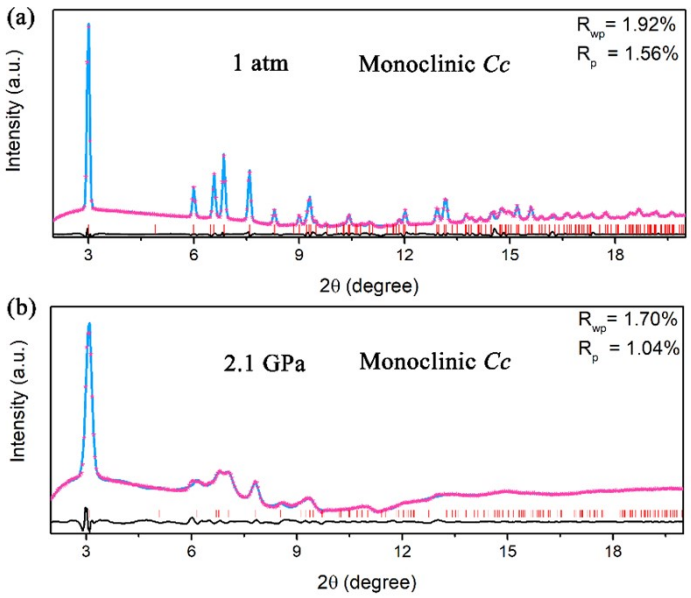

Figure S3. Rietveld refinement of the ADXRD pattern of $(2meptH_2)PbCl_4$ (a) 1atm, (b) at 2.1 GPa. Red bars reflect the refined peak positions and black line represents the difference between observed (blue) and simulated (pink) diffraction profiles.

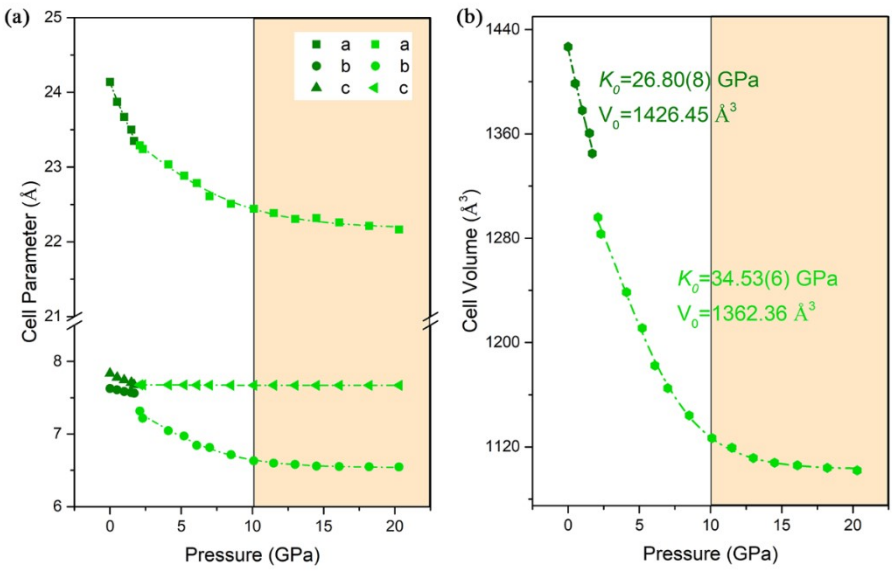

Figure S4. (a) Evolution of lattice constants of $(2meptH_2)PbCl_4$ as a function of pressure. (b) Change in unit cell volume with pressure of $(2meptH_2)PbCl_4$ upon compression. After 10.0 GPa, the lattice constant changed slowly in the shadowed part, which is caused by the significantly distorted inorganic structure.

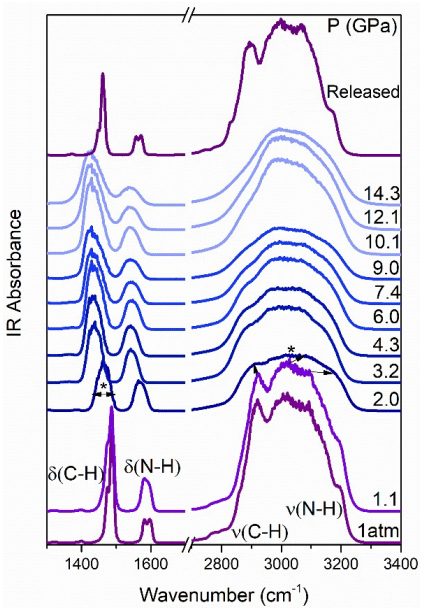

Figure S5. Infrared spectra of $(2meptH_2)PbCl_4$ as a function of pressure.

The distortion of inorganic frameworks upon compression is usually accompanied by the evolution of organic cations, so we performed *in-situ* high-pressure infrared absorption spectrometry of the samples to study the high-pressure behavior of the organic cations. As shown in Figure S5, the peak positions of the infrared absorption spectrum were identified according to previous literature reports, including the C-H bending mode (1480 cm^{-1}), the N-H bending mode (1580 cm^{-1}), the C-H stretching mode (2900 cm^{-1}) and N-H stretching mode (3180 cm^{-1}).[2] In the lower pressure region, the peak position change of the infrared spectrum is not obvious, until 2.0 GPa the peak intensity is significantly weakened. It can be seen that the vibration of organic cations

is severely inhibited by the inorganic framework, which corresponds to the volume collapse of the crystal. When the pressure continued to increase, the C-H bending mode (1480 cm^{-1}) and the N-H bending mode (1580 cm^{-1}) exhibited the most obvious red shift, which indicated the interaction between the organic cations and the inorganic framework gradual enhancement results in the enhanced twisting of organic cations.[3] As the pressure increases to 10.1 GPa, the vibrational intensities of the C-H stretching mode (2900 cm^{-1}) and the N-H stretching mode (3180 cm^{-1}) start to increase, which corresponds to the violent twisting of the inorganic octahedra. Therefore, in summary, the behavioral changes of organic cations are inextricably linked to the structural changes of inorganic octahedra.

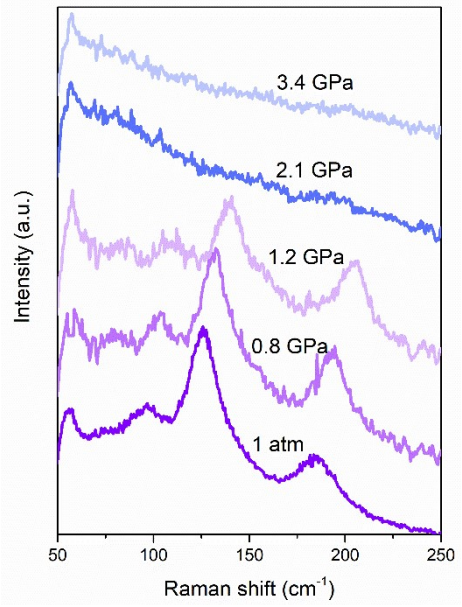

Figure S6. Raman spectra of $(2meptH_2)PbCl_4$ at selected pressures.

In the low frequency range below 80 cm^{-1}, the Raman band is related to the lattice vibration mode, and with the increase of pressure, the lattice vibration film gradually moves towards the detectable region. The lattice modes (80−180 cm^{-1}) are associated with Pb−Cl vibrational modes consisting of ionic/covalent interactions in the inorganic framework.[4-5] The dramatic weakening or even disappearance of Raman peaks below 200cm^{-1} also indicates significant deformation of octahedral perovskites at 2.1 GPa (Figure S6).

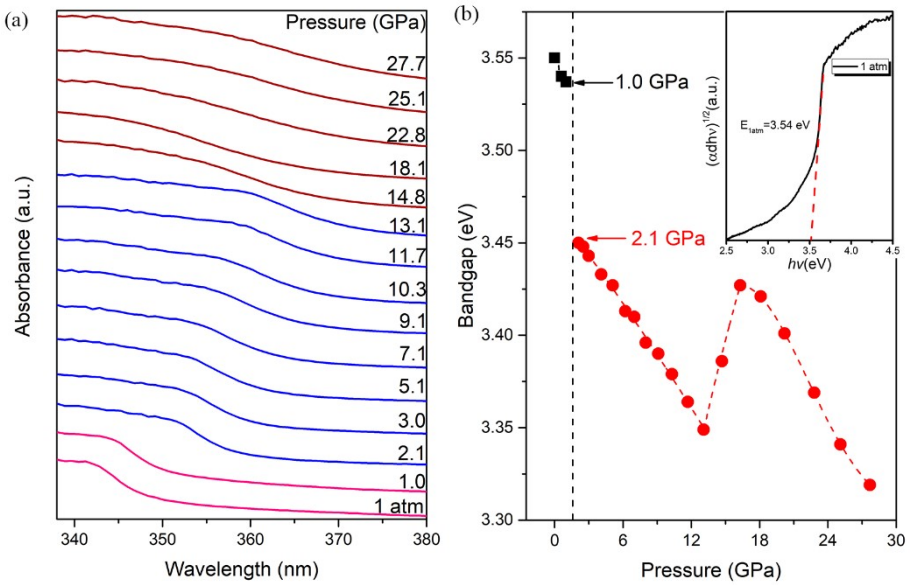

Figure S7. (a) Selected high-pressure UV/Vis absorption spectra for $(2meptH_2)PbCl_4$. (b) Band gap evolution of $(2meptH_2)PbCl_4$ under high-pressure. The inset shows a Tauc plot for$(2meptH_2)PbCl_4$ at 1 atm.

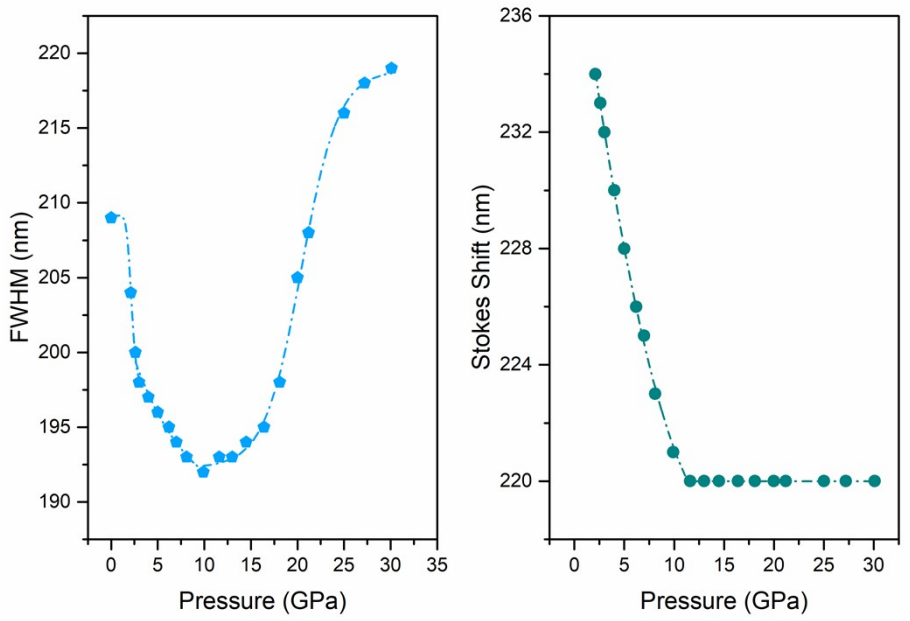

Figure S8. (a) Full width at half-maximum (FWHM) of the emission band of $(2meptH_2)PbCl_4$ crystal upon compression. (b) Pressure-induced Stokes shift change of $(2meptH_2)PbCl_4$.

Below 9.9 GPa, the Stokes shift decreases with pressure (Figure S8b), indicating that the proportion of energy absorbed for emission increased. This provides evidence for the observation that PL intensity shows significant, continuous enhancement with PL peak upon compression.

Table S2 Pressure dependence of PL intensity, Average lifetime, RPLQY, Radiative recombination rate and Non-radiative recombination rate of $(2meptH_2)PbCl_4$

Pressure (GPa)	PL intensity I/I_0	Average lifetime (ns)	RPLQY	Radiative recombination rate(ns^{-1})	Non-radiative recombination rate(ns^{-1})
0.0	1.0	3.824	0.010	0.00262	0.25889
2.1	12.0	5.418	0.116	0.02141	0.16316
3.0	20.6	6.895	0.194	0.02814	0.1169
4.0	33.1	10.711	0.321	0.02997	0.06339
5.0	50.7	13.543	0.492	0.03633	0.03751
6.2	79.5	18.093	0.771	0.04261	0.01266
8.1	129.8	23.688	1.259	0.05315	0.01093
9.9	190.7	29.513	1.850	0.06268	0.00288
13.0	169.8	31.685	1.647	0.05198	0.00304
16.4	131.4	27.632	1.274	0.04611	0.00992
18.1	93.3	20.454	0.905	0.04425	0.01464
20.0	65.1	16.768	0.631	0.03763	0.02201
25.0	19.6	13.777	0.190	0.01379	0.05879
30.1	12.9	12.567	0.125	0.00995	0.06963

1. S. Wang, Y. Yao, Z. Wu, Y. Peng, L. Li, J. Luo, *J. Mater. Chem. C.*, 2018, **6**, 12267-12272.
2. Y. Gu, K. Wang, Y. Dai, G. Xiao, Y. Ma, Y. Qiao and B. Zou, *J. Phys. Chem. Lett.*, 2017, **8**, 4191-4196.
3. L. Zhang, C. Liu, Y. Lin, K. Wang, F. Ke, C. Liu, W. L. Mao, B. Zou, *J. Phys. Chem. Lett.*, 2019, **10**, 1676-1683.
4. A. Maaej, M. Bahri, Y. Abid, N. Jaidane, Z. B. Lakhdar, A. Lautié, *Phase Transitions*, 1998, **64**, 179-190.
5. R. G. Niemann, A. G. Kontos, D. Palles, E. I. Kamitsos, A. Kaltzoglou, F. Brivio, P. Falaras, P. J. Cameron, *J. Phys. Chem. C*, 2016, **120**, 2509-2519.